fast helium atoms, it seemed most useful to use an incident beam in which equilibrium existed between the excited and ground state atoms. At the lower energies (10–20 kev) the values of σ_{10} obtained by de Heer[11] are seen to be in good agreement with the present results.

In Fig. 4, the corresponding cross sections are plotted for a target gas of helium and again a comparison is made with values obtained by other experimenters. The values of σ_{10} are in substantial agreement at higher energies with those of Allison and at lower energy there is good agreement with the values obtained by Stedeford[5]; however, the discrepancy with Krasner's results for σ_{01} is also present for helium gas. The capture or charge exchange cross section σ_{10} for helium ions in helium gas represents a resonant process in that the change in the total internal energy of the colliding particles during the collision is zero. From classical arguments, it is expected that the cross section will decrease as the relative velocity increases. From an inspection of the various σ_{10}-velocity curves, it is noted that in gases other than helium the cross section passes through a maximum, whereas in helium it decreases throughout the energy range from 4 to 200 kev. The theoretical results of Jackson.[13] Schiff,[14] and Moiseiwitsch[15] are shown as the Curves J, S, and M respectively. Using an impact-parameter method, Jackson and Moiseiwitsch have calculated the cross sections for energy less than 100 kev. The primary difference in these calculations is the form of the He_2^+ wave function used. At higher energies, the impact method is not applicable and Schiff has used an extension of the Born approximation. In the energy regions where these separate methods are appropriate, the agreements between the theoretical and experimental results are satisfactory.

The cross sections shown in Figs. 5 and 6 for the target gases nitrogen and oxygen are substantially equal except in the low-energy region where the slope of the σ_{10} curve for nitrogen is much greater than that for oxygen. These results are compared in Fig. 6 with those obtained by the Chicago group using air as the target gas. It is seen that reasonable agreement was obtained with Allison for σ_{10}, but that the σ_{01} curves differ by nearly a factor of two. For the gases neon and argon, the results are plotted in Figs. 7 and 8. No data are available for comparison at high energies, but the values obtained by Stedeford in the energy range 4 to 30 kev are in good agreement with present values.

ACKNOWLEDGMENTS

It is a pleasure to acknowledge the helpful suggestions and comments of Dr. A. H. Snell and Dr. J. L. Fowler in the performance of this work.

PHYSICAL REVIEW VOLUME 109, NUMBER 2 JANUARY 15, 1958

Hyperfine Structure Measurements on Plutonium-239*

J. C. Hubbs, R. Marrus, W. A. Nierenberg, and J. L. Worcester
Radiation Laboratory and Department of Physics, University of California, Berkeley, California

(Received September 20, 1957)

The atomic hyperfine structure of plutonium-239 has been investigated by the atomic-beam magnetic resonance method. Research has centered about a relatively highly populated electronic energy level having unit angular momentum which is probably the first excited state of a ground-state ^7F term arising from the configuration $(5f)^6\,(6d)^0\,(7s)^2$. Atomic and hyperfine structure constants for this level are found to be $I=\frac{1}{2}$, $J=1$, $g_J=1.4975\pm0.0010$, $\Delta\nu=7.683\pm0.060$ Mc/sec.

From the measured hyperfine structure separation and $5f$ wave functions derived from a Hartree relativistic calculation, the nuclear magnetic moment is inferred to be ±0.02 nm under the assumption that the $J=1$ level under investigation arises from a pure ^7F term belonging to the configuration $(5f)^6$.

INTRODUCTION

THE heavy elements, those elements toward the end of the periodic table as it is now known, are particularly interesting as a class because of the characteristic nuclear properties exhibited in this region, because of the transition-type electronic systems found here, and because of the opportunities for a more sensitive test of the relativistic theory of the atomic system.

Plutonium has been investigated previously with respect to nuclear and atomic properties by the methods of optical spectroscopy and paramagnetic resonance. Van den Berg and Klinkenberg[1] first observed the optical spectrum and found the nuclear spin to be $\frac{1}{2}$. Later Conway[2] observed the furnace spectrum reporting on approximately 500 lines; as yet no term analysis has been made. McNally and Griffin[3] have investigated

* This work was done under the auspices of the U. S. Atomic Energy Commission.

[1] M. Van den Berg and P. F. A. Klinkenberg, Physica **20**, 461 (1954).
[2] J. G. Conway, J. Opt. Soc. Am. **44**, 276 (1954).
[3] J. A. McNally and P. M. Griffin in Stable Isotopes Division

the spectrum of Pu(II) and give a preliminary term analysis of the ion. Bleaney and co-workers[4] first observed the paramagnetic resonance spectrum of Pu^{239} in certain salts and verified Klinkenberg's spin assignment. These data and information regarding the electronic structure of uranium[5,6] indicate that the electronic configuration of Pu would be either $(5f)^5\ (6d)^1$ or $(5f)^6\ (6d)^0$, with a preference for the latter.[7]

The primary objective of the research is to establish a basis for the understanding of electronic structure in the heavy-element group; this is a necessary precursor to any measurements of the more subtle nuclear properties, such as the dipole, quadrupole, and octupole moments, through atomic hyperfine structure. A secondary objective is a verification of the spin of Pu^{239}.

PRODUCTION OF AN ATOMIC BEAM

Simpson and co-workers[8] have investigated the vapor pressure of plutonium from 1100°C to 1500°C, using an effusion method and tantalum containers. Although no interaction between plutonium and tantalum was observed at these temperatures, it was found necessary to use nested sharp-edged containers to prevent liquid plutonium from creeping out the effusion orifice.

Extrapolation of the vapor-pressure data indicated that the 0.1 mm Hg required for the resonance experiments would be reached at 1650°C. At this temperature, however, it is found that satisfactory beams are not obtained from tantalum containers. The apparent vapor pressure falls rapidly, and subsequent examination shows the formation of a hard crystalline substance which is apparently a product of interaction between plutonium and tantalum. Moreover, a sharp edge on the inner crucible fails to control creep completely.

For this reason experiments were made on refractory Pu salts in the hope that one might be found that decomposes in the vapor phase at the appropriate effusion level. Compounds with carbon, silicon, and oxygen were tried without success. The results of Conway indicate substantial decomposition of the oxide at a temperature of 2500°C.[2] A measurement of the effective vapor pressure of a sample, initially PuO_2, up to a temperature of 2000°C failed to show signs of decomposition (Fig. 1). Further, the deflecting magnets proved incapable of deflecting any measurable fraction of the beam, thus establishing that decomposition does not occur at the temperature reached. A single trial with Pu metal in a carbon crucible indicated that the

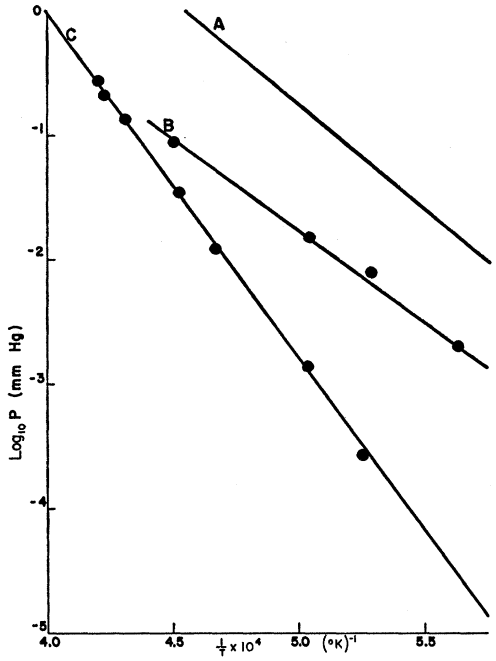

FIG. 1. Vapor pressures of plutonium compounds. Curve *A*. Vapor pressure of plutonium metal as measured by Simpson and co-workers.[8] Curve *B*. Vapor pressure of a sample initially PuSi, taken in a tantalum container. Curve *C*. Vapor pressure of a sample initially PuO_2 taken in a tantalum container. The absolute uncertainty in the data is a factor of about three. Relative values should be much better.

vapor pressure of the carbide is too low to be useful, i.e., less than 10^{-2} mm Hg at 2000°C. The silicide, formed by the interaction of metallic silicon and plutonium in tantalum containers, proved to be more tractable in the sense that a beam of atoms was formed, but the apparent vapor pressure (Fig. 1) indicates that decomposition probably occurs at the silicide-tantalum interface. This conclusion is supported by the observation that the melt does attack the tantalum, although at a rate at least an order of magnitude slower than plutonium alone. Several runs made using this system showed that approximately $\frac{1}{3}$ of an initial load of 20 to 50 mg Pu could be effused before attack became so complete as to reduce the effective effusion rate to $\frac{1}{10}$ its initial value. Attempts to maintain a constant effusion rate by increasing the temperature invariably result in lower yield because of the extreme temperature dependence of the rate of interaction.

At the same time as the above studies were being made, an investigation was made of refractory materials other than tantalum with a view toward the elimination or reduction of the creep and attack phenomena. The materials tried were tantalum, molybdenum, tungsten, thorium and cerium sulphides, and thorium oxide. Only tungsten was found to be acceptable in regard to the requirements of availability, freedom from interaction, and nonporosity. Ultimately, a satisfactory beam was achieved with tungsten containers, as illus-

Semiannual Progress Report for Period Ending November 30, 1956, Oak Ridge National Laboratory Report ORNL-2236, February, 1957 (unpublished).

[4] Bleaney, Llewellyn, Pryce, and Hall, Phil. Mag. **45**, 773 (1954).

[5] Kiess, Humphrey, and Laun, in National Bureau of Standards Report, NBS-A 1747, 1944 (unpublished).

[6] P. Schurmans, Physica **11**, 419 (1946).

[7] E. K. Hyde and G. T. Seaborg, Handbuch der Physik, Vol. 34 (to be published).

[8] Phipps, Sears, Seifert, and Simpson, in *Proceedings of the International Conference on Peaceful Uses of Atomic Energy, Geneva, 1955* (United Nations, New York, 1956), Vol. 7, p. 382.

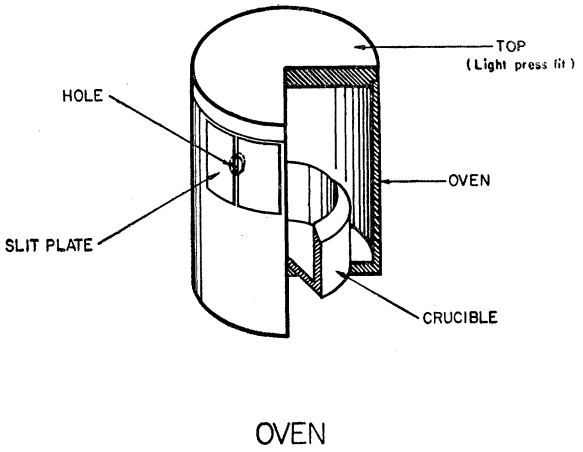

FIG. 2. Cutaway view of ovens used for the production of a plutonium beam. The body, cap, and inner crucible are machined from solid tungsten stock, and the slit jaws, of 3-mil tantalum foil, are spot-welded to the body.

trated in Fig. 2. The liquid melt is contained in an inner cup with a sharp lip, the inner cup being isolated from the outer (which determines the beam geometry) by a barrier of cerium or thorium sulphide or of thorium oxide. The relatively small transfer rate via the vapor phase is handled by the application of a large temperature gradient to the outer crucible. Since creep takes place selectively in the direction of the temperature gradient, and since the inner container is at an average temperature, back-evaporation keeps the melt in the inner crucible. It is also found that the sharp lip on the inner crucible is alone sufficient to prevent creep from the slit jaws. In this way beams of plutonium are produced for periods as long as 15 hours and at vapor pressure up to 0.5 mm Hg, the Knudsen limitation for the particular beam geometry. The effective effusion rate at constant temperature is characterized by a slow monotonic drop to approximately one-half the initial value and then a sharp decrease over a period of less than 2 minutes as the oven is finally exhausted. The empty crucible, when examined, shows no sign of attack, with the occasional exception of the slit jaws, which—because they must be spot-welded on—are thin

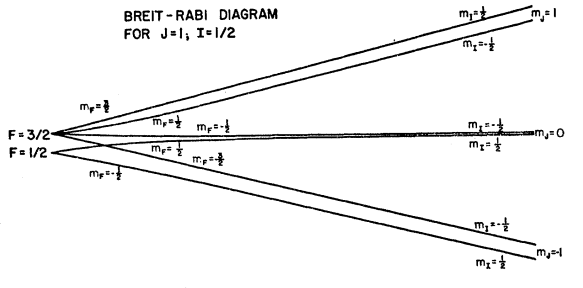

FIG. 3. Energy levels of the $J=1$ state of Pu^{239} in a magnetic field, hyperfine structure assumed to be positive. Since no measurement is made of the sign of the hyperfine structure the transitions referred to in the text are labeled under this assumption.

tantalum foil. The apparent vapor pressure during the initial stages of the beam is in good agreement with an extrapolation of the data of Simpson *et al.*

ENERGY LEVELS IN A MAGNETIC FIELD

The Hamiltonian describing an atom with angular momentum $J\hbar$, magnetic moment $g_J\mu_0\mathbf{J}$, and a nucleus with angular momentum $I\hbar=\frac{1}{2}\hbar$, magnetic moment $g_I\mu_0\mathbf{I}$, in a magnetic field H is

$$\mathcal{H}=A\mathbf{I}\cdot\mathbf{J}-g_J\mu_0\mathbf{J}\cdot\mathbf{H}-g_I\mu_0\mathbf{I}\cdot\mathbf{H}, \qquad (1)$$

where A is the hyperfine-structure constant. This Hamiltonian is identical to that used in the derivation of the Breit-Rabi[9] formula, which applies to the case $J=\frac{1}{2}$, $I=I$. Therefore, by interchange of I and J, the energy levels of Pu^{239} in a magnetic field are given by

$$\frac{W}{\Delta W}=-\frac{1}{2(2J+1)}-\frac{mg_J\mu_0H}{\Delta W}\pm\tfrac{1}{2}\left(1-\frac{4mx}{2I+1}+x^2\right)^{\frac{1}{2}},$$

where $x=(g_J-g_I)\mu_0H/\Delta W$, $\Delta W=a(J+\frac{1}{2})$, and $g_J<0$ for electrons. The energy levels are shown in Fig. 3.

BEAM DETECTION

Plutonium can be detected by the surface ionization method, by the detection of alpha and gamma particles emitted in natural decay, and by the detection of stimulated fission events in large neutron fluxes. Alpha-particle detection is used because of its relative simplicity and the availability of large quantities of plutonium.

The thermal neutral plutonium beam is allowed to fall on a platinum foil, which is freshly flamed before being placed in the apparatus, and which is introduced to and removed from the apparatus via a vacuum lock. The collection efficiency of such surfaces for beams of Am, Pu, and U is at least 25%, probably unity, and highly reproducible. Foils so exposed to the beam are counted in 2π alpha counters with backgrounds between 0.07 and 0.15 count per minute except for occasional bursts due to line noise. A typical resonance run is

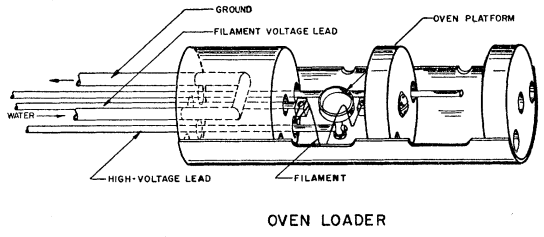

FIG. 4. High-temperature electron-bombardment oven system. The oven (Fig. 2) is placed in the cup and the unit capped with a matching semicylinder which serves as a heat shield. The unit shown is only the head of a more elaborate oven loader which allows the oven to be put into the apparatus without disturbing the can vacuum.

[9] G. Breit and I. I. Rabi, Phys. Rev. 38, 2082 (1931).

made over a period of 4 to 12 hours with an exposure taken every 5 minutes. The beam is run at such a level that resonance points yield a count rate of 1 to 2 counts per minute. Preliminary count rates are obtained during the run, and the final data are obtained by repeated counting in a bank of three to six counters over a period of several days to a week. In all cases at least three long counts are made on each point to eliminate data taken during a temporary high-background interval. The research reported here is based on more than 1000 exposures taken in this manner.

APPARATUS AND PROCEDURE

The atomic beam apparatus used in the investigation has been described elsewhere[10]; the only essential modification has been the incorporation into the buffer chamber of a movable potassium oven which serves as beam flag and field calibrator. Intercalibration of potassium from this source and cesium from a source at the plutonium oven position shows no significant position- or velocity-dependent resonance shift for C fields between 0 and 50 gauss.

The observed potassium resonance is symmetric, with a half-width between 70 and 90 kc/sec. A mean measurability of the C field under operating conditions is about 5 milligauss and the mean change in C field over a 5-minute exposure is about 2 milligauss; these effects introduce a 15-kc/sec mean uncertainty in the position of the plutonium resonance; therefore plutonium resonances are taken with points separated by 25 to 50 kc/sec. Field calibration is performed every 15 to 20 minutes, and the mean field at any exposure period is determined by a straight-line extrapolation between nearest calibration points.

The high-temperature electron-bombardment oven system, which has not been previously described, is detailed in Fig. 4. Heat transfer and freedom from outgassing are excellent up to an oven temperature of 2000°C which is reached, for the standard oven design, with an expenditure of about 200 watts.

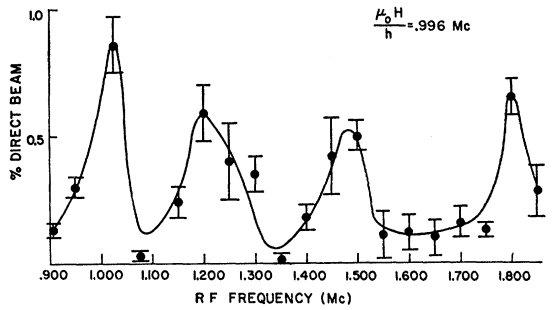

FIG. 5. Results of a very-low-field search to obtain information regarding the electronic ground state of plutonium. The resonance at 1.0 Mc/sec is ascribed to a $J=1$, $F=\frac{3}{2}$ state for which $g_J=1.5$, whereas the resonances at 1.2, 1.8, and 1.5 Mc/sec are ascribable to the $F=\frac{5}{2}$ and $F=\frac{3}{2}$ states of $J=2$ and to a contaminant with $I=0$, respectively, all states having g_J about 1.5. The size of the 1.5-Mc/sec resonance is compatible with the known level of Pu^{240} contamination, but no proof can be made on the basis of decay because of the similarity of the Pu^{239} and Pu^{240} alpha spectra.

[10] Brink, Hubbs, Nierenberg, and Worcester, Phys. Rev. **107**, 189 (1957).

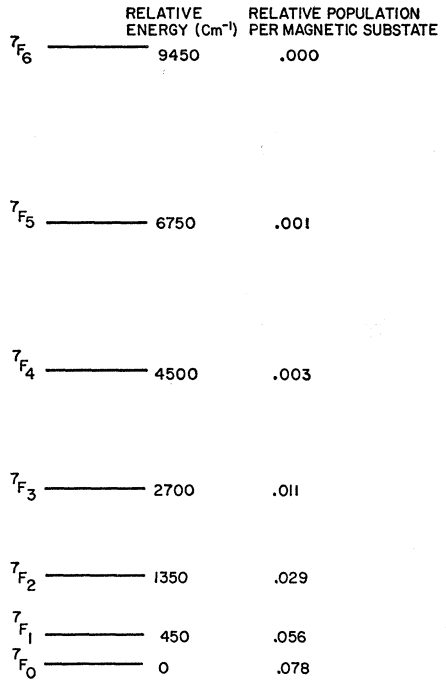

FIG. 6. Assumed ^7F level structure in Pu^{239}. The approximate fine-structure splitting constant is deduced from optical data in U(I), U(II), and Am(III). The diagram is used for illustrative purposes only and no connection with the quantitative features of the actual situation is inferred. The relative population of each level per magnetic substate is calculated for 1685°C, at which temperature beams of plutonium are made.

EXPERIMENTAL DATA

An initial plutonium search taken with a C field below 1 gauss was made to obtain information regarding the electronic ground state of plutonium. Resonances are found at frequencies corresponding to g values of 1.0, 1.2, 1.5, and 1.8 (Fig. 5); the electronic state is

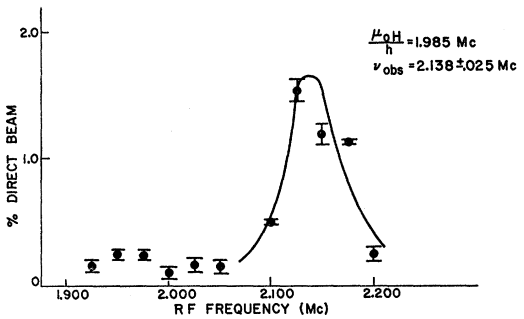

FIG. 7. Plutonium resonance at about 1.4 gauss which, together with Fig. 5, indicates that the level under investigation has an extremely small hyperfine structure. In this, as in all following data presentation, the value of the magnetic field is quoted to one milligauss and the uncertainty in the field value is absorbed into the uncertainty in resonance frequency.

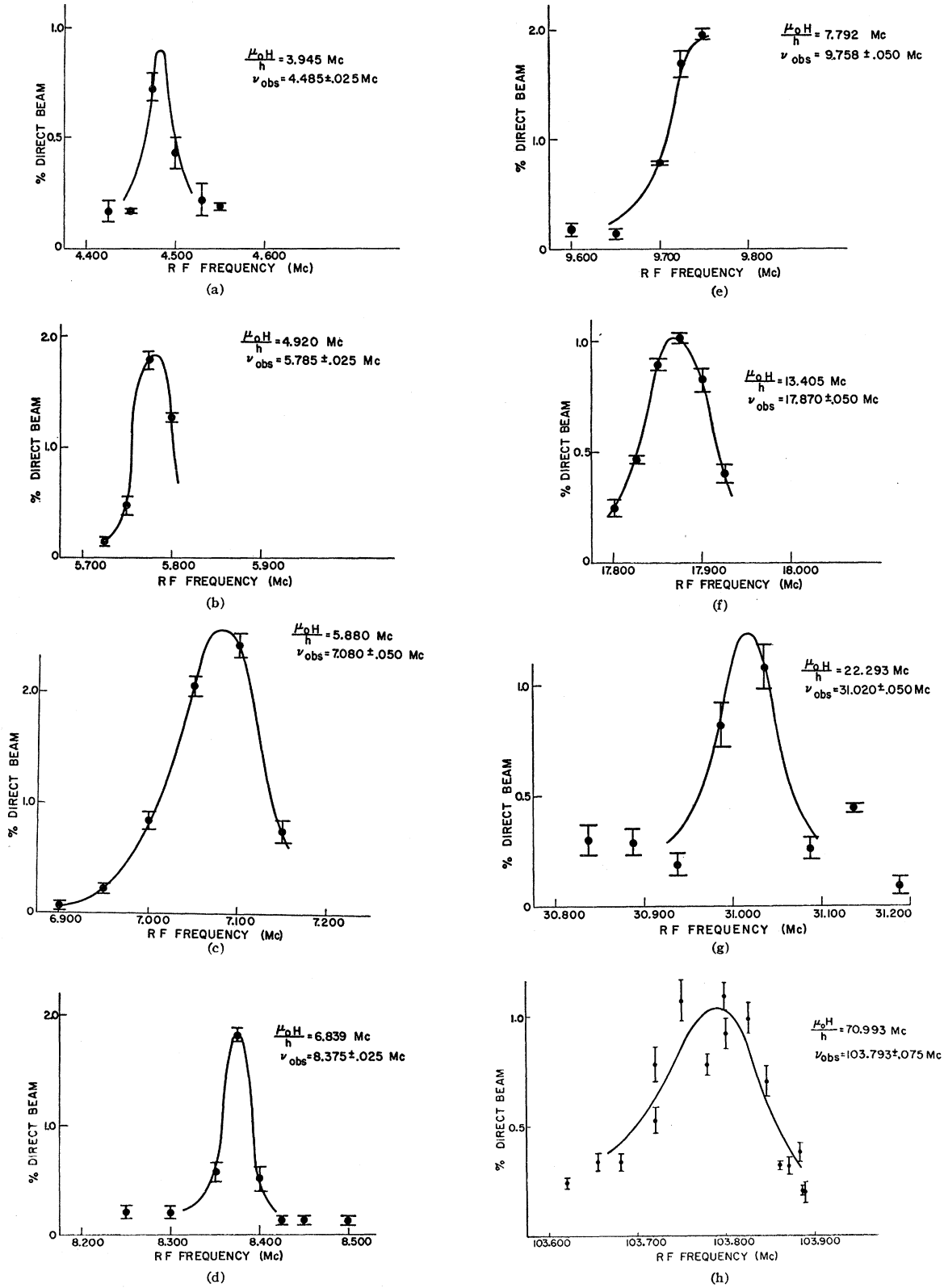

FIG. 8. Observations of the $J=1$, $F=\frac{3}{2}$, $M_F=\frac{1}{2}\leftrightarrow M_F=-\frac{3}{2}$ double-quantum transition (Fig. 3) through intermediate field and into the Paschen-Back region. The uncertainties in each case are assigned values based on C-field drift and on the data. Most of the time additional points were taken at either side of the resonance and in some instances the observations were repeated.

strongly intimated to be ^7F, the only probable assignment for which we have $g_J=\frac{3}{2}$ for $J=1$ and 2, and the Hund's rule ground-state term for one of the two preferred configurations,[7] $(5f)^6$. The fine-structure splitting constant for this term is known, from U(I), U(II), and Pu(II) data, to be about 450 cm^{-1}, and the sample is known to contain 5% to 10% Pu^{240} by activity, giving the central resonance (1.5 Mc/sec). Concluding that no appreciable gains were to be made by improvements in the precision and reliability of this data, we concentrated immediately on the strongest observed transition, that one corresponding to $g_F=1$ and presumed to arise from the $J=1$ first excited state (Fig. 6), and the $F=\frac{3}{2}$ level ($I=\frac{1}{2}$).

Further observation of the $F=\frac{3}{2}$ state at 1.4 gauss (Fig. 7) showed a large quadratic shift characteristic of an extremely small hyperfine-structure separation. Because it is expected that all levels of the ^7F multiplet have comparable hyperfine structure separations, and since the $J=2$ and $J=3$ states are expected to be appreciably populated at beam temperatures, the complexity of intermediate-field line structure is considerable. Therefore, the $J=1$, $F=\frac{3}{2}$ line was followed at small field increments through the intermediate field region to 5.6 gauss (Fig. 8) near the Paschen-Back region. The observed resonance intensity serves as a further aid to identification.

These data were first fitted to the transition $F=\frac{3}{2}$, $M_F=-\frac{1}{2}\rightarrow M_F=-\frac{3}{2}$ (Fig. 3). This transition was used to fit the observations because the separation of the lines $M_F=-\frac{1}{2}\leftrightarrow M_F=-\frac{3}{2}$ and $M_F=\frac{1}{2}\leftrightarrow M_F=-\frac{1}{2}$ is, in this region, about 500 kc/sec, and because an off-center geometry was used which is designed to refocus this transition in first order. Subsequent finding of the transition $F=\frac{3}{2}$, $M_F=\frac{1}{2}\leftrightarrow F=\frac{1}{2}$, $M_F=-\frac{1}{2}$ (Fig. 9) near 8 Mc/sec and further observations in the Paschen-Back region (Fig. 8) showed, however, that all observations have made on the double-quantum transition $F=\frac{3}{2}$, $M_F=\frac{1}{2}\leftrightarrow M_F=-\frac{3}{2}$, which results in a change in sign of the effective magnetic moment in the deflecting fields. Since the resonances are customarily observed at rf amplitudes about six times "optimum," the only unexpected result, on the basis of conventional double-quantum treatments, is that full flop is observed with a difference between single quantum frequencies of about ten times the natural line width. The line width observed is 40 to 60 kc/sec in comparison with the 60 to 80 kc/sec predicted from K^{39} transitions, in good agreement with the theory of the double-quantum process. The double-quantum assumption was verified by repetition of several of the intermediate field points with a standard flop-in beam geometry which discriminates against the $F=\frac{3}{2}$, $M_F=-\frac{1}{2}\leftrightarrow M_F=-\frac{3}{2}$ transition by at least one order of magnitude. In each case the transition intensity was found to be about the average 1.5%.

All observations of the $M_F=\frac{1}{2}\leftrightarrow M_F=-\frac{3}{2}$ transition are summarized by Fig. 10, which presents the difference between calculated and observed frequencies as a function of magnetic field. No corrections have been made in the calculation for the small third-order shift,

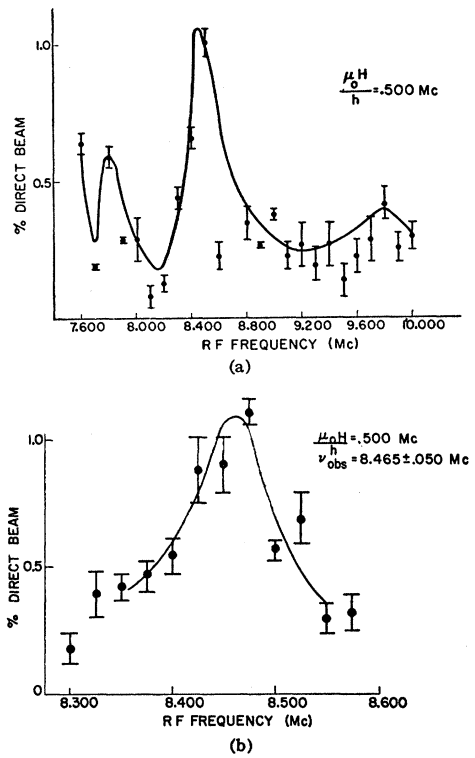

FIG. 9. (a) Data obtained during the search for $\Delta F=\pm 1$ transitions at low field. The resonance near 8.5 Mc/sec is due to the transition $F=\frac{3}{2}$, $M_F=\frac{1}{2}\leftrightarrow F=\frac{1}{2}$, $M_F=-\frac{1}{2}$ (Fig. 3); the effect around 7.7 Mc/sec is probably due to transitions normally forbidden by apparatus selection rules but allowed in first order by an off-center geometry used in this search. (b) Detail of the transition $F=\frac{3}{2}$, $M_F=\frac{1}{2}\leftrightarrow F=\frac{1}{2}$, $M_F=-\frac{1}{2}$ (Fig. 3) on which the hyperfine-structure assignment is based.

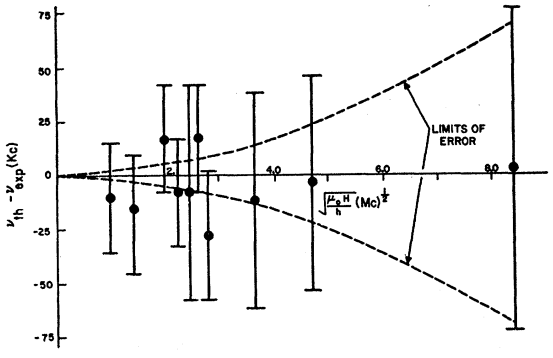

FIG. 10. Summary of all resonance data on the $F=\frac{3}{2}$ double-quantum transition. The ordinate is the difference between calculated and observed resonance frequencies (in kc/sec), while the abscissa is proportional to $H^{\frac{1}{2}}$, a convenient scale for the points taken. The dotted line shows the permissible range of observations for the given uncertainty in g_J only. A discrepancy between the assumed and correct values of ΔW in excess of 60 kc/sec would cause most of the resonance centers to fall above or below the horizontal axis.

since it should be completely masked by uncertainties in the observed line position. The uncertainties given for each measurement are determined by inspection of individual resonance curves, with a 15-kc/sec minimum uncertainty set by C-field variations and a maximum set by the appearance of the resonance itself, the object being to determine a mean uncertainty. It would appear that the stated values are rather more generous than would be the mean. The dotted curves show the allowable range of observations for the stated uncertainty in the value of g_J.

THEORY

A. Electronic g Factor

The Landé g factor for a pure nonrelativistic unshielded ^7F term, including the anomalous magnetic moment of the electron,[11] is

$$g_J=(g_L+g_S)/2=1.50115.$$

The first-order value must be corrected for the following effects: (a) the deviation of the term from the Russell-Saunders limit, arising from fine structure; (b) configuration mixing; (c) higher-order relativistic effects, including the bound-state and radiative terms[12]; (d) an effect that may be interpreted as a diamagnetic shielding[13] of the valence electrons and is generally included in (c), but is here considered separately. Effect (d) is estimated to be comparable to the observed effect and to be much larger than (c); accordingly a calculation of the shielding effect is planned. For the present one can say only that the combined effects of (a) and (b) on the g factor is less than 1%.

B. Hyperfine-Structure Separation

The hyperfine-structure constant A, defined by Eq. (1), is essentially the product of the nuclear magnetic moment and a magnetic field at the nucleus arising from the electronic system. That is, since we define $\mathcal{H}=A\mathbf{I}\cdot\mathbf{J}$, and because for the first-order magnetic dipole interaction we have $\mathcal{H}=-g_I\mu_0\mathbf{H}\cdot\mathbf{I}$, we obtain $A=-g_I\mu_0H/J$. This magnetic field is susceptible to calculation but is, in general, complicated by the fact that the valence electrons may not be describable by functions of a single configuration. The observed g_J value suggests, however, that the assumption of Russell-Saunders coupling arising from a single configuration may be valid for the case under investigation. A calculation of the hyperfine-structure constant has therefore been made under these assumptions, and neglects the breakdown of strict $L-S$ coupling for relativistic wave functions. With these assumptions we require, for appropriately symmetrized wave functions corresponding to the configuration $(5f)^6$ and the term ^7F, matrix elements of the z component of magnetic field at the nucleus which are diagonal in the total angular momentum, J. The magnetic field operator in symmetrized form is

$$\mathbf{H}=\sum_i \mathbf{H}_i=\sum_i\left(\frac{e\mathbf{v}\times\mathbf{r}}{r^3}+\frac{\boldsymbol{\mu}(\mathbf{r}^2)-3\mathbf{r}(\boldsymbol{\mu}\cdot\mathbf{r})}{r^5}\right)_i$$
$$=\sum_i\{a\mathbf{l}+b[\mathbf{s}(\mathbf{l}^2)-\tfrac{3}{2}\mathbf{l}(\mathbf{l}\cdot\mathbf{s})+(\mathbf{l}\cdot\mathbf{s})\mathbf{l}]\}_i. \quad (2)$$

The matrix elements of this field can be calculated by straightforward application of this operator to the appropriately symmetrized wave functions of the electronic system. This procedure is very tedious, however, and offers little insight into the physical situation. Another method is the calculation by general arguments of the matrix elements, which are diagonal in J and M_J, of the magnetic field for an arbitrary electronic state in Russell-Saunders coupling. The appropriate constants of the general form for the Hund's rule ground-state term of equivalent electrons can be expressed in closed form. The necessary numerical applications are made to the state $(5f)^6\ ^7F$, for plutonium.

The total orbital and spin angular momenta, L and S respectively, are assumed to be good quantum numbers. Therefore the matrix elements of the individual momenta diagonal in L and S are

$$\begin{aligned}\langle LM_L|\mathbf{l}_i|LM_L'\rangle&=C_L\langle LM_L|\mathbf{L}|LM_L'\rangle,\\ \langle SM_S|\mathbf{S}_i|SM_S'\rangle&=C_S\langle SM_S|\mathbf{S}|SM_S'\rangle,\end{aligned} \quad (3)$$

where, by equivalence of the electrons, there is no i dependence of the C's. By the usual vector coupling rules, the appropriate matrix elements of the magnetic field reduce to

$$\langle JMLS|\mathbf{H}|JMLS\rangle$$
$$=\left\{A\frac{\mathbf{L}\cdot\mathbf{J}}{\mathbf{J}^2}+B\left[3\frac{(\mathbf{L}\cdot\mathbf{J})(\mathbf{L}\cdot\mathbf{S})}{\mathbf{J}^2}-\frac{\mathbf{L}^2(\mathbf{S}\cdot\mathbf{J})}{\mathbf{J}^2}\right]\right\}\langle|\mathbf{J}|\rangle. \quad (4)$$

The J, M_J dependencies of the matrix elements of the magnetic field have now been removed. There remains only the evaluation of the coefficients A, B for an arbitrary number of equivalent electrons coupling to the Hund's rule ground-state term. To accomplish this we return to the individual electron form, Eq. (2), which is applied to the state $J=M_J=L+S$.

The matrix elements of the z component of the magnetic field at the nucleus which are diagonal in the

[11] P. Kusch and H. M. Foley, Phys. Rev. **74**, 250 (1948).
[12] G. Breit, Nature **122**, 649 (1928); Phys. Rev. **34**, 553 (1929); **39**, 616 (1932).
[13] W. E. Lamb, Jr., Phys. Rev. **60**, 817 (1941).

individual electron coordinates l_i, s_i, m_{li}, and m_{si} are

$$\langle lsm_lm_s|\mathbf{H}_Z|lsm_lm_s\rangle$$
$$=-2\mu_0\left\langle l\left|\frac{1}{r^3}\right|l\right\rangle\sum_i\{\langle lm_l|\mathbf{l}_Z|lm_l\rangle$$
$$+\langle sm_s|\mathbf{s}_z|sm_s\rangle\langle lm_l|1-3\cos^2\theta_l|lm_l\rangle\}_i$$
$$=-2\mu_0\left\langle l\left|\frac{1}{r^3}\right|l\right\rangle\sum_i\left[m_l+\frac{2m_s}{(2l-1)(2l+3)}\times(3m_l^2-l(l+1))\right]. \quad (5)$$

The wave function for the state $J=M_J=L+S$ is, for a shell that is less than half filled,

$$\psi^{J,J}=\frac{1}{(n!)^{\frac{1}{2}}}\sum_P(-1)^P[u_1(m_l=l,\ m_s=\tfrac{1}{2})\times u_2(m_l=l-1,\ m_s=\tfrac{1}{2})\cdots\times u_n(m_l=l-n+1,\ m_s=\tfrac{1}{2})], \quad (6)$$

where the u's are wave functions for the individual electrons in the states l, m_l, $s=\frac{1}{2}$, m_s, and the permutations P may be taken over electrons or states.

Application of Eqs. (5) and (4) to the wave function (6) gives

$$\langle L+S,\ L+S|\mathbf{H}_Z|L+S,\ L+S\rangle$$
$$=-2\mu_0\left\langle l\left|\frac{1}{r^3}\right|l\right\rangle\left\{L+\frac{1}{(2l-1)(2l+3)}[-nl(l+1)+3l^2+3(l-1)^2+\cdots+3(l-n+1)^2]\right\}$$
$$=-2\mu_0\left\langle l\left|\frac{1}{r^3}\right|l\right\rangle\left[L+\frac{L(2L-n^2)}{n(2l-1)(2l+3)}\right] \quad (7a)$$
$$=AL+B[LS(2L-1)]. \quad (7b)$$

Equation (7b) results from Eq. (4) evaluated for the state $J=L+S$, $M_J=L+S$.

The treatment is extended to shells which are more than half filled by identification of the wave function (6) as a wave function for n missing electrons. It is thus found that for n equivalent electrons (or n missing electrons) coupling to the Hund's rule ground-state term $S=\frac{1}{2}n$, $L=\frac{1}{2}n(2l-n+1)$ in Russell-Saunders coupling, the hyperfine-structure constants are given by

$$A(J)=+2g_I\mu_0^2\left\langle l\left|\frac{1}{r^3}\right|l\right\rangle\left\{\frac{J(J+1)+L(L+1)-S(S+1)}{2J(J+1)}+\frac{2(2L-n^2)}{n^2(2L-1)(2l-1)(2l+3)}\left[\frac{L(L+1)[J(J+1)+S(S+1)-L(L+1)]}{2J(J+1)}-\frac{3}{4}\frac{[J(J+1)-L(L+1)-S(S+1)][J(J+1)+L(L+1)-S(S+1)]}{J(J+1)}\right]\right\}. \quad (8)$$

The number of electrons, or of missing electrons, n, is of course less than or equal to $2l+1$.

For the ^7F_J level of $(5f)^6$, Eq. (8) gives

$$A(J)=g_I\mu_0^2\left\langle\frac{1}{r^3}\right\rangle_{5f}\left\{\frac{J(J+1)+58}{90}\right\},$$
$$A(^7F_1)=g_I\mu_0^2\times\tfrac{2}{3}\left\langle\frac{1}{r^3}\right\rangle_{5f}. \quad (9)$$

The value of $\langle 1/r^3\rangle$ appropriate to $5f$ electrons is estimated from Dirac wave functions calculated for uranium by a Hartree procedure.[14] Values of $\int[(F^2+G^2)/r^3]dr$ and $\int[FG/r^2]dr$ are determined by numerical integration of the wave functions on the IBM 650. The results are

$$\text{“}\left\langle\frac{1}{r^3}\right\rangle_{f_{\frac{1}{2}}}\text{”}=\frac{1}{2\alpha a_0}\int\frac{FG}{r^2}dr=3.89a_0^{-3},$$
$$\left\langle\frac{1}{r^3}\right\rangle_{f_{\frac{5}{2}}}=\int\frac{F^2+G^2}{r^3}dr=3.99a_0^{-3}.$$

The ratio of these two is the relativistic correction factor. It is thus evident that for $5f$ electrons relativistic contributions to the hyperfine-structure constant are not important in the Hartree approximation.

The hyperfine-structure constant is therefore, under the foregoing assumptions,

$$A=g_I\mu_0^2\times\tfrac{2}{3}\times\frac{3.89}{a_0^3}=124g_I\ \text{Mc/sec}.$$

The observed hyperfine-structure constant is

$$A=2\Delta W/3=\pm5.14\ \text{Mc/sec}.$$

Therefore, the magnetic moment of Pu^{239} is inferred to be

$$\mu=g_II=\pm2.1\times10^{-2}\ \text{nm}.$$

The inferred magnetic moment is so different from that estimated by Bleaney[4] and co-workers that it is well worth while to consider other possible sources of information. In regard to $\langle 1/r^3\rangle$, an estimate may be

[14] S. Cohen (private communication).

made from fine structure through[15]

$$A_{fs}=\frac{e^2}{2m^2c^2}\left\langle\frac{1}{r}\frac{dV}{dr}\right\rangle, \quad \mathcal{H}=A_{fs}\mathbf{L}\cdot\mathbf{S}. \tag{10}$$

Assuming the potential to be essentially $Z_{eff}e^2/r$ in regions of greatest contribution to the average, we obtain

$$A_{fs}=2Z_{eff}\mu_0^2\left\langle\frac{1}{r^3}\right\rangle=5.84Z_{eff}\left\langle\frac{a_0}{r}\right\rangle^3 \text{ cm}^{-1}. \tag{11}$$

Conway[16] has observed a fine-structure splitting constant for Am^{+++} in $LaCl_3$ in the ^7F term of 450 cm^{-1}, and we estimate 760 cm^{-1} for the fine-structure splitting constant of the ^4I term in U(I) and U(II). These values predict a fine-structure splitting constant for $5f$ electrons of 2700 cm^{-1} and 2280 cm^{-1} for Am and U respectively, so that from Eq. (11) we predict

$$\langle 1/r^3\rangle \simeq (4.5/a_0^3)\times(Z_{eff}/Z),$$

in good agreement with our derived value of $1/r^3$ and reasonable values of Z_{eff}/Z for $5f$ electrons.

We also may crudely estimate the nuclear magnetic moment of Pu^{239} from the work of Klinkenberg,[1] who finds hyperfine-structure separations in the spectra of plutonium averaging about 50 cm^{-1}, and the work of Fred and Tompkins[17] on Am^{241} and Am^{243}; they find total hyperfine structures for configurations containing S electrons averaging about 1500 cm^{-1}. Since the total hfs widths are directly proportional to the magnetic moment, for magnetic dipole interactions, and since Fred estimates reliably that $\mu_{Am}=1.4$, Klinkenberg's work intimates a magnetic moment on the order of 0.05 nm.

FURTHER OBSERVATIONS INDIRECTLY CONCERNING THE ELECTRONIC STRUCTURE OF PLUTONIUM

Data having a direct and unambiguous connection with the electronic structure of plutonium have been presented. Other observations have, however, been made that have indirect bearing on the subject:

1. The mean fraction of the beam involved in the $J=1$ resonance is 1.5%. Empirically determined resonance factors predict a $J=1$ state population of 6% ±3% per magnetic substate. The assumption of a ^7F term obeying the interval rule and with a fine-structure splitting constant of 450 cm^{-1} would give 5.6% (Fig. 5).

2. The mean fraction of the beam involved in a Majorana transition at zero C field is about 3%. The prediction of the assumptions of Fig. 5 is 2.6%.

3. The fraction of the beam that is not thrown out by the A and B fields is 62±5%. This consists of fast atoms, atoms in the state $M_J=0$, and most of any molecules in the beam. Using for the first term an empirical value of 5% of atoms not in the state $M_J=0$ and assuming the absence of molecules, we estimate that 60% of the beam is in the $M_J=0$ state. The prediction according to the above assumptions is 40%.

SUMMARY

The nuclear spin of Pu^{239} is observed to be $\frac{1}{2}$, and a low-lying electronic state is observed to have unit angular momentum with g value 1.4975±0.0010. This g factor and observed beam intensities are clearly consistent with the assumption that the $J=1$ level is the first excited state of the ground-state term ^7F. This term is, in turn, the Hund's rule ground state for the configuration $(5f)^6$, the preferred configuration for plutonium from optical spectroscopic investigations of U(I), U(II), and Pu(II).

The magnitude of the g factor implies that the $J=1$ level is very close to the $L-S$ coupling limit. This result would be predicted from the fact that the first excited term in samarium, the rare earth analogous to Pu, lies 14 000 cm^{-1} above the ground state,[18] and that a ^7F fine-structure constant of 450 cm^{-1} is predicted for plutonium.

ACKNOWLEDGMENTS

It is with pleasure that we acknowledge the generous assistance, invaluable advice, and encouragement given us by B. B. Cunningham and J. C. Wallmann of the Physical Chemistry Group. Without their aid, especially in the early stages of the research, this investigation would not have been possible.

[15] E. U. Condon and G. H. Shortley, *The Theory of Atomic Structure* (Cambridge University Press, Cambridge, 1935), p. 120.
[16] J. G. Conway (private communication).
[17] M. Fred and F. S. Tompkins, J. Opt. Soc. Am. (to be published).
[18] W. E. Albertson, Phys. Rev. **47**, 370 (1935); **52**, 644 (1937).